The Electronic Structure of Carbon Nanotubes with Finite Length : Tight Binding Theory

Won-Ha Moon*, Won-Woo Kim, and Ho-Jung Hwang

Department of Electrical and Electronic Engineering, Chung Ang University, Seoul 156-756, Korea

E-mail : siryu011@korea.com

(Received 19 November 2001, Accepted 9 February 2002)

The electronic properties of Carbon Nanotube(CNT) are currently the focus of considerable interest. In this paper, the electronic properties of finite length effect in CNT for the carbon nano-scale device is presented. To Calculate the electronic properties of CNT, Empirical potential method (the extended Brenner potential for C-Si-H) for carbon and Tight Binding molecular dynamic (TBMD) simulation are used. As a result of study, we have known that the value of the band gap decreases with increasing the length of the tube. The energy band gap of (6,6) armchair CNT have the ranges between 0.3 eV and 2.5 eV. Also, our results are in agreements with the result of the other computational techniques.

Keywords : Carbon nanotube, Tight binding method, Brenner hydrocarbon potential

1. INTRODUCTION

Since their discovery in 1991 by Iijima[1], Carbon Nanotubes (CNT) have been the subject of intensive experimental and theoretical efforts. It has been known that CNTs are metallic, while others are semiconducting, depending on their diameter and chirality[2-4]. As the diameter decreases, The band gap of CNT is increased. Also the (n, n) armchair nanotube is metallic while (n, 0) zigzag nanotube is semiconducting dependent of the chirality which can be uniquely determined by the chiral vector (n, m), where n and m are integers[5-7]. The scanning tunneling microscopy (STM) studies of single wall carbon nanotube (SWNT) have confirmed this predicted behavior.

Understanding the dependence of the electronic structure of CNT on their lengths, diameters, and chiralities is of vital importance for their possible use in nanoelectronics applications[8]. Where CNTs could be used as junctions, bends, or the building blocks of transistors and electron emitters of nanometer dimensions[9]. In this paper, we have taken 2 steps to investigate the electronic properties of finite length effect in CNTs with cap. (i) First, we have applied the extended Brenner (XB) potential for C-Si-H to simulate CNTs with cap. (ii) Secondly, TBMD has been applied to study the electronic properties of CNTs with finite length such as density of states (DOS). As a result of study, we have known that the value of the band gap decreases with increasing the length of the tube. The energy band gap of (6,6) armchair CNT have the ranges between 0.3 eV and 2.5 eV. Also as the length of CNT is less than 20Å, its energy band gap is fluctuated sensitively.

2. COMPUTATIONAL METHODS

2.1 Extended Brenner (XB) potential for hydrocarbon

The reliability of atomistic Mote Carlo and molecular dynamics simulation techniques that have impacted areas ranging from drug design to crystal growth – depends on the use of appropriate interatomic energies and forces. These have traditionally been derived from classical interatomic potentials, or more recently from first principles or semi empirical electronic structure techniques[10]. While the latter approaches are becoming more prevalent due to increasing computer resources and clever algorithms, there remain clear advantages to classical potentials for large systems and long simulation times.

Using classical molecular dynamics (MD) simulations

with XB potential for C-Si-H[11], we investigate the possibility of the CNTs with cap. The empirical hydrocarbon potential was developed by Brenner in order to model CVD diamond growth. It has since been successfully applied to many other systems involving carbon and hydrogen, including fullerenes. The Brenner potential is of the cluster-functional type, and it takes into account the chemical environment of the atoms as well as their geometrical relationships with one another. Important aspects of carbon chemistry, such as bond conjugation and bond order, and treated by the Brenner potential via the inclusion of specially fitted bond order correction terms. Here we simply summarize the relevant mathematical expressions.

The binding energy is given as a sum over bonds as

$$E_b = \sum_i \sum_j [V_R(r_{ij}) - \overline{B_{ij}} V_A(r_{ij})] \quad (1)$$

Where the repulsive and attractive pair terms are given by

$$V_R = f_c(r_{ij})[D_{ij}^{(e)}/(S_{ij}-1)\cdot\exp[-\sqrt{2S_{ij}}\,\beta_{ij}(r_{ij}-R_{ij}^{(e)})]] \quad (2)$$

and

$$V_A = f_c(r_{ij})[D_{ij}^{(e)} S_{ij}/(S_{ij}-1)\cdot\exp[-\sqrt{2/S_{ij}}\,\beta_{ij}(r_{ij}-R_{ij}^{(e)})]] \quad (3)$$

The cut off function $f_c(r)$ restricts the pair potential to nearest neighbors. The empirical bond order function is given by

$$\overline{B_{ij}} = \frac{1}{2}[B_{ij}^{-\delta_{ij}} + B_{ij}^{-\delta_{ji}} + F_{ij}(N_i^{(t)}, N_j^{(t)}, N_{ij}^{conj})] \quad (4)$$

where

$$B_{ij} = 1 + \sum_{k(\neq i,j)} G_i(\theta_{ijk}) f_c(r_{ik}) \cdot \exp\{\alpha_{ijk}[(r_{ij}-R_{ij}^{(e)})-(r_{ik}-R_{ik}^{(e)})]\} + H_{ij}(N_i^H, N_i^C) \quad (5)$$

and

$$G(\theta) = a_0\{1 + c^2/d^2 - c^2/[d^2+(1+\cos\theta)^2]\} \quad (6)$$

and the function F and H are the bond order correction terms. With the exception of the F and H bond order correction terms. The complete parameter set for the extended Brenner potential is given in Table 1. The coordination number for a certain carbon atom is given as the sum of the cut-off function over all of its neighbors,

$$N_i = \sum f_c(r_{ij}), \quad (7)$$

where the cut-off function is defined as

$$f_c(r) = \begin{cases} 1, & r < R_{ij}^{(1)} \\ \frac{1}{2}[1+\cos(\frac{\pi(r-R_{ij}^{(1)})}{(R_{ij}^{(2)}-R_{ij}^{(1)})})], & R_{ij}^{(1)} < r < R_{ij}^{(2)} \\ 0, & r > R_{ij}^{(2)} \end{cases} \quad (8)$$

The bond order correction terms(F and H) utilize the coordination number N_i in order to determine the local bonding. It is vital that the cut-off distances are chosen with this in mind. This can be simply illustrated by considering the case of an acetylene molecule Initially there is a triple-bond between the carbon atoms of the molecule. As one of these carbon atoms moves within the cut-off distance, the resulting increase in N_i indicates that the carbon-carbon bond should become a double bond. The bond energy for a carbon-carbon double bond is less than that for a triple bond, so there is an increase in the potential energy of the molecule as the re-hybridization occurs. Chemically, this is a result of a new bond forming between the carbon atoms, and the energy of the new bond more than compensates for the energy lost in the re-hybridization. However, if the cut-off distances are too large, the coordination number will increase before the new bond has formed. This is clearly unphysical, and results in nonsensical reaction paths. The cut-off distances were carefully chosen to avoid such problems.

To investigate the accuracy of the calculation reported in this paper, the atomization energy of hydrocarbon molecules are presented in Table 2. Ab initio HF calculations using the fairly sophisticated 6-311+g(3df,2p) and 6-311++g basis sets, and including correlation effects at either the MP2 or MP4 level, are observed to overestimate the atomization energies by as much as 20%. The less sophisticated ab initio HF calculations, using the 3-2lg* basis set and including exchange and correlation effects via the Becke3LYP functional , yield results which differ from those of the more rigorous calculations by 6% or less. These results indicate that there is little to be gained in going beyond the Becke3LYP/3-21g* level in performing the HF/DFT

Table 1. Parameters for the XB potential for carbon.

$R_{ij}^{(e)}$	1.315 Å	$D_{ij}^{(e)}$	6.325eV
	1.5 Å^{-1}		1.29
	0.80469		0.0 Å^{-1}
$R_{ij}^{(1)}$	1.7 Å	$R_{ij}^{(1)}$	2.0 Å
	0.011304		361
	6.25		

Table 2. Atomic energy (in eV) determined form the X3 potential. Ab initio HF/DFT calculation and experiment.

Molecule	XB	Beck3 LYP3-21g*	MP2 6-311++g	Exp	
C_2H_2	17.1	20.9	21.3	17.1	[12]
CH_3	12.7	15.2	14.9	12.8	[12]
CH_4	17.6	20.1	19.6	17.6	[12]

calculations. They also suggest that the binding energies obtained by performing ab initio Becke3LYP/3-21g* HF/DFT calculations may be too high by as much as 25%.

2.2 Empirical tight binding model for carbon

In this paper, we investigated the electronic properties of CNTs with finite length using the tight binding approach. This is useful to enhance the understanding of realistic carbon nanotubes. The tight binding (TB) technique used in this study was described in detail elsewhere[13], where it was already shown to be of usefulness in handling carbon fullerenes, and so on.

First principles studies have obtained accurate and reliable results. Nevertheless, they are at present still limited by their heavy demand on computational effort. Also most of empirical potential models are classical in nature and cannot account for quantum mechanical effects of the bonding in carbon systems. An alternative approach is to include the effects of directional covalent bonding through the underlying electronic structure described by an empirical TB Hamiltonian. Such a scheme allows the quantum mechanical nature of the covalent bonding to enter the potential in a natural way rather than through the addition of *ad hoc* angular terms in classical potentials.

In this paper, we applied empirical tight binding potential for carbon by C.H Xu et al for the dependence of the TB hopping parameters and the pairwise potential on the interatomic separation. In this model the total energy of the system is written as

$$E_{tot} = E_{bs} + E_{rep} \tag{9}$$

where *Ebs* is the sum of electronic eigenvalues over all occupied electronic states, and *Erep* is a short-ranged repulsive energy. The electronic eigenvalues are obtained by solving an empirical tight binding Hamiltonian H_{TB}. The off-diagonal elements of H_{TB} are described by a set of orthogonal sp3 tow-center hopping parameters, $V_{ss\sigma}, V_{sp\sigma}, V_{pp\sigma}$ *and* $V_{pp\pi}$, scaled with interatomic separation *r* as a function *s(r)*; and the on-site elements are the atomic orbital energies of the corresponding atom. The remainder of *Etot* is modeled by a short-ranged repulsive term *Erep* given by

$$E_{rep} = \sum_i f\left(\sum_j \phi(r_{ij})\right) \tag{10}$$

where $\phi(r_{ij})$ is a pairwise potential between atoms *i* and *j*, and *f* is a functional expressed as a 4th-order polynomial with argument $\sum_j \phi(r_{ij})$. We adopt the functional form suggested by GSP[11] for the scaling function *s(r)* and the pairwise potential $\phi(r_{ij})$

$$s(r) = (r_0/r)^n \exp\{n[-(r/r_c)^{n_c} + (r_0/r_c)^{n_c}]\}$$
$$\phi(r) = \phi_0 (d_0/r)^m \exp\{m[-(r/d_c)^{m_c} + (d_0/d_c)^{m_c}]\} \tag{11}$$

where r0 denotes the nearest-neighbour atomic separations in diamond, and *n, nc, rc, φ0, m, dc* and *mc* are parameters that need to be determined. Unlike in the GSP model, the scaling parameters *rc* and *nc* for *s(r)* are not necessarily the same as the corresponding *dc* and *mc* for *φ(r)* in our model. Moreover, for the convenience of molecular dynamics simulation, we require the scaling function *s(r)* and the pair potential *φ(r)* to go smoothly to zero at some designated cut off distance. This is achieved by re replacing the tail of *s(r)* with a third order polynomial $t_s(r-r_l)$ whose coefficients are determined by requiring the connection of *s(r)* and $t_s(r)$ at r_l (match point, $r_l<r_m$) to be smooth up to the first derivative, and $t_s(r)$ and its first derivative to be zero at r_m. The same procedure is used to determine $t_c(r-d_l)$, which replaces the tail of *φ(r)*. This model chose the cut off distance *rm* and *dm* to be 2.6Å, which is between the nearest neighbour and next nearest neighbour distances of carbon atoms in the diamond structure at equilibrium. The parameters in the model are chosen primarily by fitting first principles LDA results of energy versus nearest neighbour interatomic separation for different carbon polytypes, i.e. diamond, graphite, linear chain, simple cubic and face-centered cubic structures, with special emphasis on the diamond, graphite and linear chain structures. Additional checks have also been made to ensure that the model gives reasonable results for the electronic band structure, elastic moduli and phonon frequencies in the diamond and graphite structures, although these properties do not enter explicitly into the fitting procedure. The resulting sp3 tight binding parameters are: E_s = *-2.99eV*, E_p = *3.71eV*, $V_{ss\sigma} = -5.0eV, V_{sp\sigma} = 4.7eV, V_{pp\sigma} = 5.5eV, V_{pp\pi} = -1.55eV$. The parameter for *s(r)* and *φ(r)*, the coefficients for the tail functions $t_s(r-r_l)$ and $t_c(r-d_l)$, and the coefficient for the polynomial function $f(x) = \sum_{n=0}^{4} c_n x^n$, with $x = \sum_j \phi(r_{ij})$ are given in Table 3 and Table 4.

Table 3. Parameters for the functions $s(r)$ and $\phi(r)$.

n	n_c	r_c(Å)	R_0(Å)	R_1(Å)	
2.0	6.5	2.18	1.536329	2.45	
ϕ_0(eV)	m	m_c	d_c(Å)	D_0 (Å)	D_1(Å)
8.18555	3.30304	8.6655	2.1052	1.64	2.57

Table 4. Coefficient of the polynomial functions $t_s(r-r_1)$, $t_e(r-d_1)$, $f(x)$.

	$t_s(r-r_1)$	$t_e(r-d_1)$	$f(x)$
c_0	6.7392620074314*10-3	2.2504290109*10-8	-2.5909765118191
c_1	-8.1885359517898*10-2	-1.4408640561*10-6	0.5721151498619
c_2	0.1932365259144	2.1043303374*10-5	-1.78963499039996*10-3
c_3	0.3542874332380	606024390226*10-5	2.35392215167 57*10-5
c_4			-1.24251169551587*10-7

These parameters produce excellently the energy curves of the two most stable structure, i.e. graphite and diamond[14].

In conclusion, TB model gives an accurate description of the atomic interactions in carbon systems. It is able to reproduce to energy-volume curve of accurate LDA calculations, with excellent transferability among the graphite, diamond and linear chain structures.

3. RESULTS AND DISCUSSION

Figure 1 shows (6, 6) armchair CNT with 264 carbon atoms before simulation. The processing time of CNT with cap changes sensitively as the temperature changes. Fig. 2 shows process of making CNT with cap for 4.5 ps in 3000 K.

We have investigated the processing time of CNT with cap, as compared with bonding energy and defect numbers. It is shown in Figure 2 that the bonding energy, with defect numbers, is reduced to 3.2 ps. The CNT structure is comparatively stable after 3.2ps.

The bonding energy and defect numbers in 3000K and 4000K is shown in Fig. 3 and 4. The processing time of CNT with cap decreases as the temperature increases. As Figure 4 shows the processing time of CNT with cap is 2.4 ps in 4000K. It is also observed that the processing

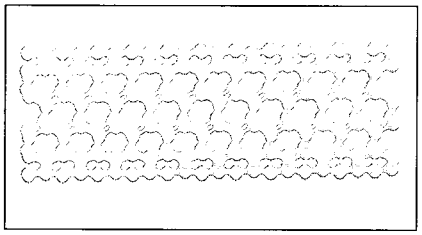

Fig. 1. (6,6) armchair CNT before simulation.

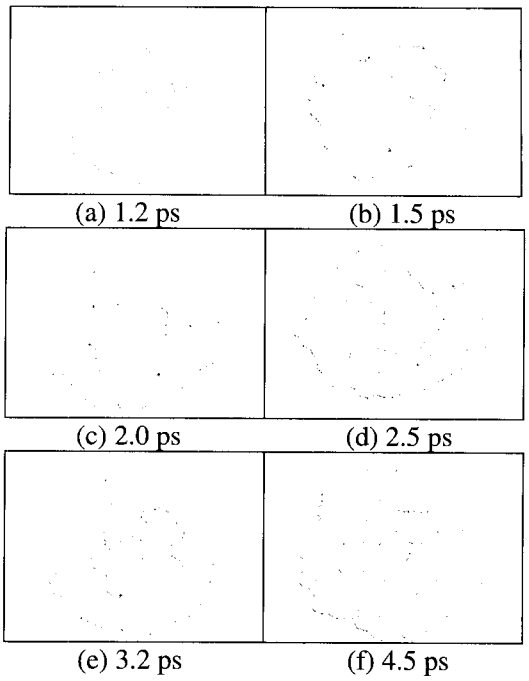

Fig. 2. Simulation of CNT capping process.

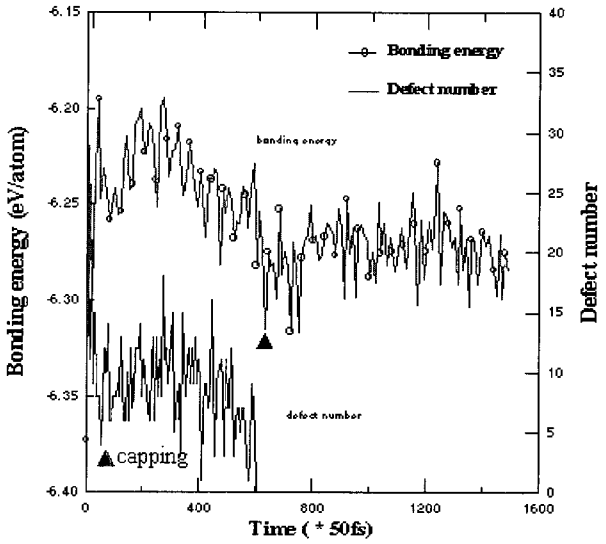

Fig. 3. Bonding energy and defect numbers in 3000K.

time in 3000K increases 0.8ps, as compared with 4000K.But the relaxation and contraction of CNT occurs in 300K, 2000K. Figure 5 shows the dependence of bonding energy on the temperature. The bonding energy increases as the temperature increases. Because CNT is being stable for the process of capping, the bonding energy decreases. Also the boding energy increases again in about 2000K for breaking carbon-carbon interaction. Figure 6 shows the optimized structure of (6, 6) carbon nanotube with cap using the conjugate gradient method.

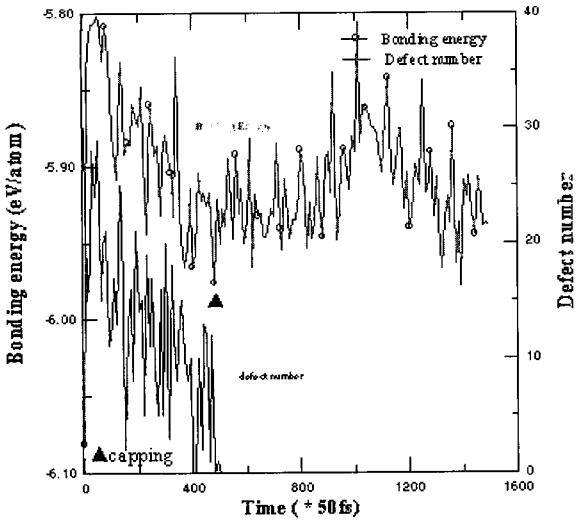

Fig. 4. Bonding energy and defect numbers in 4000K.

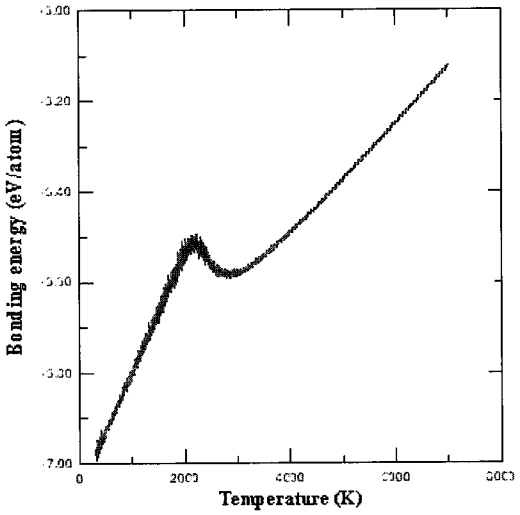

Fig. 5. Bonding energy of CNT in 300K-7000K.

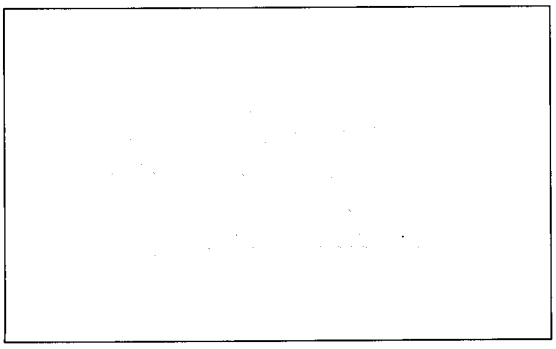

Fig. 6. The optimized structure of (6, 6) single wall carbon nanotube (SWNT).

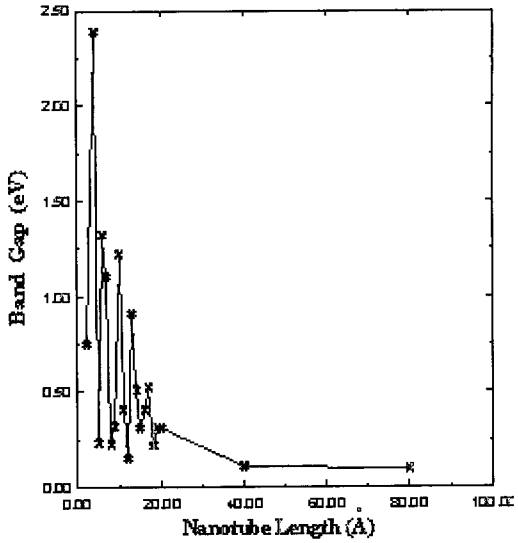

Fig. 7. Variation of the band gap as a function of the length.

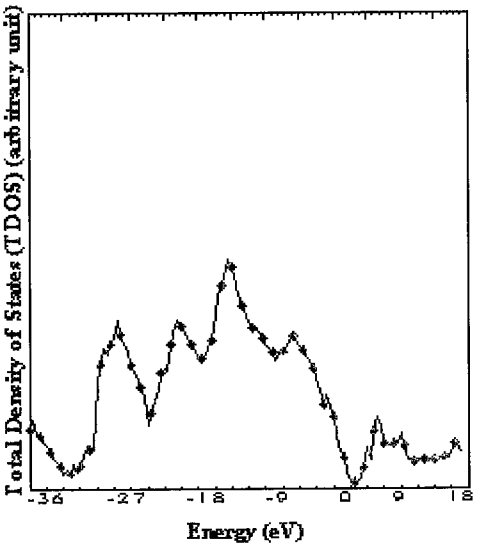

Fig. 8. Total Density of States (TDOS) of (6,6) SWNT.

The electronic properties of finite length effect in (6,6) SWNT with cap were calculated using TBMD. As a result of TBMD simulation, the band gap decreases as the length of CNT increases. However, the decrease is not monotonic but shows a well defined oscillation in short tubes. Finite size graphite are known to have a finite band gap, but no oscillation is observed. In Fig. 7, TB model used predicted that, unlike the infinite tube that is metallic, very short nanotube has the band gap. The band gap shows a regular oscillatory dependence on tube length. The band gap values varies from 0.3 to 2.5 eV for tubes shorter than 20 Å. This oscillation is explained for effect of π-bonding between carbon and arbon. It is also observed that CNT, longer than 40 Å,

have the properties of the metal. Figure 8 shows total density of states(TDOS) of (6, 6) SWNT. This explain the metallic behavior of (6, 6) SWNT is metallic. Band gap oscillations were also reported by Yoshizawa et al. For 2-D polyphenanthrenes on the basis of extended Huckel band structure calculations[15].

Finally, we have compared the variation of the band gap using ab initio: Hatree-Fock (HF) and Density Functional Theory (DFT), and semi empirical: Modified Neglect of Differential Overlap-Parameterized Model 3 (MNDO-PM3) and extended Huckel (EHMO) computational methods in Fig. 9[16]. It is in agreement with the result of TBMD simulation. But both HF and MNDO-PM3 methods give a large band gap from 2.8 to 9.0 eV for 20 Å CNT[16]. The band gap values are overestimated by several electron volts for low band gap polymers due to the poor description of unoccupied orbital energy levels[17,18].

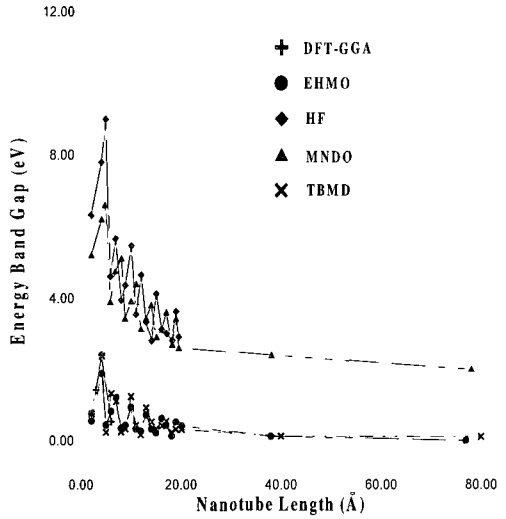

Fig. 9. Band gap using the other method (Ab initio and semi empirical method)[16].

4. CONCLUSION

We have investigated the electronic structure of finite length SWNT with cap. To Calculate the electronic properties of CNT, Empirical potential method (the extended Brenner potential for C-Si-H) for carbon and Tight Binding molecular dynamic (TBMD) simulation are used. As a result of the simulation, The processing time of making CNT with cap changes sensitively as the temperature changes. The processing time of CNT with cap is 2.4 ps in 4000K. It is also observed that the processing time in 3000K increases 0.8ps, as compared with 4000K. But the relaxation and contraction of CNT occurs in 300K, 2000K. We have also known that the value of the band gap decreases with increasing the length of the tube. However, the decrease is not monotonic but shows a well defined oscillation in short tubes. The energy band gap of (6,6) armchair CNT have the ranges between 0.3 eV and 2.5 eV for tubes shorter than 20 Å. Also, our results are in agreements with the results of the other computational techniques.

REFERENCES

[1] S. Iijima, "Helical microtubules of graphite carbon", Nature, Vol. 56, p. 354, 1999.

[2] K. S. Kim, H. J. Ryu, and G. E. Jang, "A study on the growth of carbon nanotubes using icpcvd and their field emission properties", J. of KIEEME(in Korean), Vol. 14, No. 10, p. 850, 2001.

[3] S. H. Jeong, G. E. Jang, and H. J. Ryu, "Growth of carbon nanotubes depending on ething condition of ni-catalytic layer", J. of KIEEME(in Korean), Vol. 14, No. 9, p. 751, 2001.

[4]Y. H. Lee, "Hydrogen storage in carbon nanotubes", Bulletin of KIMMEE, Vol. 13, No. 5, p. 39, 2000.

[5] J. W. Mintmire, B. I. Dunlap, and C. T. White, "Are fullerene tubules metallic?", Phys. Rev. Lett., Vol. 68, p. 631, 1992.

[6] R. Saito, M. Fujita, G. Dresselhaus, and M.S. Dresselhaus, "Electronic structure of graphene tubules based on C60", Phys. Rev. B, Vol. 46, p. 1804, 1992.

[7] B. I. Dunlap, "Relating carbon tubules", Phys. Rev. B, Vol. 49, p. 5643, 1994.

[8] M. S Dresselhaus, "Carbon nanotubes", Phys. World, 1998.

[9] M. Menon and D. Srivastava, "Carbon nanotube t junctions: nanoscale metal semiconductor metal contact devices", Phys. Rev. Lett., Vol. 79, p. 4453, 1997.

[10] M. Menon and R. E. Allen, "New technique for molecular dynamic computer simulations: hellmann feynman theorem and subspace hamiltonian approach", Phys. Rev. B, Vol. 33, p. 7099, 1986.

[11] A. J. Dyson and P. V. Smith, "Extension of the Brenner empirical interatomic potential to C-Si-H systems", Surface Science., Vol. 355, p. 140, 1996.

[12] D. W. Brenner, "Empirical potential for hydrocarbons for use in simulating the chemical vapor deposition of diamond films", Phys. Rev. B, Vol. 42 p. 9458, 1990.

[13] E. Salonen, K. Nordlund, J. Keinonen, and C. H. Wu, "Bond breaking mechanism of sputtering", Europhys. Lett., Vol. 52, p. 504, 2000.

[14] S. Fahy and S. G. Louie, "High pressure structural and electronic properties of carbon", Phys. Rev. B,

Vol. 36, p. 3373, 1987.
[15] K. Yoshizawa, K. Yahara, K. Tanaka, and T. Yamabe, "Bandgap oscillation in polyphenanthrenes", J. Phys. Chem., Vol. 102, p. 498, 1998.
[16] A. Rochefort, D. R. Salahub and P. Avouris, unpublished, 1998.
[17] W. J. Hunt and W. A. Goddard, "Excited states of H2O using improved virtual orbitals", Chem. Phys. Lett., Vol. 3, p. 414, 1969.
[18] U. Salzner, P. G. Pickup, R. A. Poirier, and J. B. Lagowski, "An accurate method for obtaining band gaps in conducting polymers using a dft/hybrid approach", J. Phys. Chem., Vol. 102, p. 2572, 1998.